Advances in Nanoparticles, 2016, 5, 53-59
Published Online February 2016 in SciRes. http://www.scirp.org/journal/anp
http://dx.doi.org/10.4236/anp.2016.51006

Preparation and Characterization of SnO_2 Nanofibers via Electrospinning

Rashmi Rani, Seema Sharma*

Ferroelectric Research Laboratory, Department of Physics, A. N. College, Patna, India
Email: *seema_sharma26@yahoo.com

Received 4 September 2015; accepted 12 February 2016; published 15 February 2016

Abstract

Tin oxide (SnO_2) nanofibers are successfully prepared by electrospinning homogeneous viscous solutions of tin acetate in polyvinylpyrrolidone (PVP). The electrospinning is carried out by applying a DC voltage to the tip of a syringe and maintaining the tip to collector distance (TCD), *i.e.* at DC electric field of 1.25 kV·cm^{-1}. The electrospun nanofibers are calcined between 550˚C and 650˚C for 4 h. Both spun and heat treated nanofibers are characterized by X-ray diffraction (XRD), transmission electron microscopy (TEM), Fourier transform infra red spectroscopy (FTIR) etc. XRD analysis of calcined nanofibers confirms the formation of pure tin oxide. TEM study showed that fibers have a polycrystalline structure with multiple nano-grains.

Keywords

Naonofibers, TEM, Electrospinning, PVP

1. Introduction

One-dimensional (1D) nanomaterials have stimulated great interest due to their importance in basic scientific research and potential technological applications [1]-[3]. It is generally accepted that 1D nanostructures are ideal systems for exploring a large number of novel phenomena at the nanoscale and investigating the size and dimensionality dependence of structure properties for potential applications [4]. 1D nanomaterials are also expected to play an important role as both interconnects and functional units in fabricating electronic, optoelectronic, electrochemical, and electromechanical devices with nanoscale dimensions [5]. Among the inorganic semiconductor nanomaterials, 1D metal oxide nanostructures are the focus of current research efforts in nanotechnology since they are the most common minerals on the Earth due to their special shapes, compositions, and chemical, and physical properties.

Tin oxide is an n-type wide band gap semiconductor and it is being used in a variety of applications such as gas sensors [6] [7] and optoelectronic devices [8] [9]. SnO_2 gas sensors give a conductance change according to

*Corresponding author.

How to cite this paper: Rani, R. and Sharma, S. (2016) Preparation and Characterization of SnO_2 Nanofibers via Electrospinning. *Advances in Nanoparticles*, **5**, 53-59. http://dx.doi.org/10.4236/anp.2016.51006

the chemical interaction between the reducing/oxidizing gases and surface adsorbed species. To enhance the gas response, the particle size needs to be decreased to the thickness level of the electron depletion layer [10] [11]. However, the strong agglomeration between primary particles often hampers the diffusion of analyte gas toward the entire sensing surface, which decreases the gas response [12] [13]. The properties of SnO_2 in various forms such as nanoparticles [14], nanowires [15], nanobelts [16] and other one-dimensional nanostructures have been extensively studied. In comparison with solid one-dimensional nanomaterials, nanotubes gain the advantages in practical applications to catalysts and gas sensors, owing to their higher surface-to-volume ratio. Moreover, the previous studies have been suggested that, the nanostructure's surface plays a significant role in defining their conductivity. Generally, the conventional methods for preparing SnO_2 nanotubes by self assembly [17] and templates directed process [18] often suffer from strict synthesis conditions or tedious procedures. Electrospinning has been considered as a simple and efficient method for producing polycrystalline nanofibers from a rich variety of materials including TiO_2 [19], SnO_2 [20], WO_3 [21], SnO_2-TiO_2 bi-component nanowires [22], MoO_3 [23], ZnO [24], and metal modified TiO_2 nanofibers [25]. However, templates and the co-electrospinning technique [26] had to be used for forming inorganic nanotubes. A one-step method for the fabrication of SnO_2 nanofibers by directly annealing electrospun composite nanofibers has been presented in this work.

2. Experiment

2.1. Chemicals and Materials

Stannic chloride pentahydrate ($SnCl_4 \cdot 5H_2O$), ethanol and N,N-dimethylformamide (DMF), Polyvinylpyrrolidone (PVP, *M*w = 1,300,000 $g \cdot mol^{-1}$) were purchased from Sigma Aldrich.

2.2. Instruments

The X-ray diffraction was from RigakuMinifiex, Japan and the transmission electron microscopy (TEM) was from JEOL, JEM-2010. The FT-IR spectra were PerkinElmer, USA.

2.3. Preparation of SnO_2 Nanofibers

Transparent spinning solution was prepared by adding 3 g of $SnCl_4 \cdot 5H_2O$ into 10 wt% PVP in ethanol/DMF solvent mixture (weight ratio 1:1), and the weight ratio of PVP and $SnCl_4 \cdot 5H_2O$ was also 1:1, followed by magnetic stirring at ambient temperature for 24 h. Later, as-prepared solution was introduced in 10 ml syringe with a hypodermic needle (dia. 2 mm) in a controlled electrospinning setup. The flow rate and applied electric field was varied to obtain the optimal conditions for the electrospun fibers. The obtained optimal condition was as follows: flow rate 0.2 ml/h and the applied electric field 1.25 kV/cm. High electric field strength (1.4 kV/cm) was employed to enable for the high stretch rates of the electrospun jet. The distance between the needle tip and the collector against the applied electric field was set as 18 cm. The longer distance between the needle tip and the collector aided the stretching of the jet due to the increase in the distance covered by the spiraling electrospun jet before being deposited on the collector. The fiber mesh obtained was then annealed to obtain SnO_2 nanofibers. The electrospun fibers were calcined at 550˚C - 650˚C for 4 h.

2.4. Characterization of the Fabricated Materials

The fine calcined powders were used to characterize the structural and microstructural properties of the compound. The X-ray diffraction pattern of the compounds were recorded at room temperature using X-ray powder diffractometer with CuKα (α = 1.5418 Å) radiation in a wide range of Bragg angles 2θ ($20^\circ \leq 2\theta \leq 70^\circ$) at a scanning rate of $2^\circ\ min^{-1}$. The structures of the electrospun nanofibers were observed by transmission electron microscopy, Spectroscopic characterization has been investigated by a Fourier-transform infrared (FT-IR) spectrophotometer.

3. Results and Discussion

3.1. Characterization of the Fabricated Materials

3.1.1. XRD Analysis

Figure 1 shows that the XRD pattern of the SnO_2 nanofiber calcined at ~600˚C for 4 h. It can be seen that all the

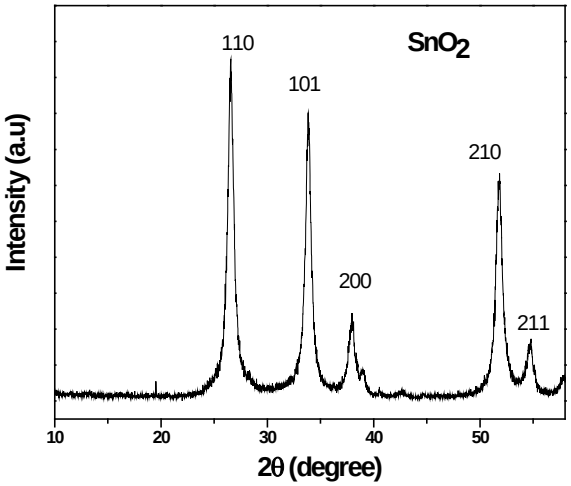

Figure 1. XRD pattern of SnO_2 nanofibers calcined at 600˚C for 4 h.

diffraction lines are assigned to tetragonal cassiterite crystalline phase of tin oxide (JCPDS card No. 77- 0452).

No characteristic peaks of impurities were observed, indicating the high purity of the products. This figure shows the electrospun SnO_2 fibers crystallized into the cassiterite structure with primary (110), (101), and (200) crystallite orientations. For the as-prepared SnO_2 nanofiber, by using Scherrer's formula,

$$D = K * \lambda / \beta_{2\theta} \cos\theta \quad (1)$$

(where D is the mean grain size, K (=0.94) is the Scherrer's constant related to the shape and index (h.k.l) of the crystal, θ is diffraction angle and λ is the X-ray wavelength used CuKα, 1.54056 Å, $\beta_{2\theta}$ is broadening of diffraction lines measured at half of its maximum intensity (in radian)). We estimated that the average grain size was about 11 nm. The lattice parameters were calculated from POWD software for the tetragonal crystal structure and were found to be

A = 7.5650 Å, c = 15.0642 Å, c/a = 1.9913 Å

3.1.2. TEM Analysis

Figure 2(a) shows the transmission electron microscopy (TEM) image of the nanofibers after calcination, indicating that the fibers were formed through the agglomeration in small beadforms. The average particle size of SnO_2 nanofiber observed in TEM image was computed to be 11.731 nm (**Figure 2(b)**) through the statistical distribution calculation.

The selected area electron diffraction (SAED pattern **Figure 2(c)**) shows characteristic crystalline planes of the SnO_2 nanofibers indicated the polycrystalline nature of SnO_2nanofiber. Inter-planar spacing (also known as d-spacing) was calculated using Bragg equation (Bragg and Bragg 1931):

$$d_{hkl} = \lambda L / R \quad (2)$$

where, R (in mm) is the radius of diffraction pattern, L (320 mm) is the distance between specimen and photographic film and λ (0.02736 Å) is the wavelength of the electron based on the accelerating voltage (200 kV).

The calculated values for d-spacings (d_{hkl}) (3.27 and 2.69 Å) were found consistent with the values from standard JCPDS File No. 77-0452 for SnO_2 (**Table 1**). Subsequently, two distinct diffraction planes were indexed as (110) and (101) facets which correspond to the tetragonal phase of tin oxide.

Figure 3 shows the Williamson Hall plot of the SnO_2nanofiber indicating crystalline strain of the material is about 0.04221. It relies on the principle that the approximate formulae for size broadening, β_L, and strain broadening, β_e, vary quite differently with respect to Bragg angle, θ:

$$P_L = K\lambda / L\cos\theta \quad (3)$$

$$\beta_e = C \in \tan\theta \quad (4)$$

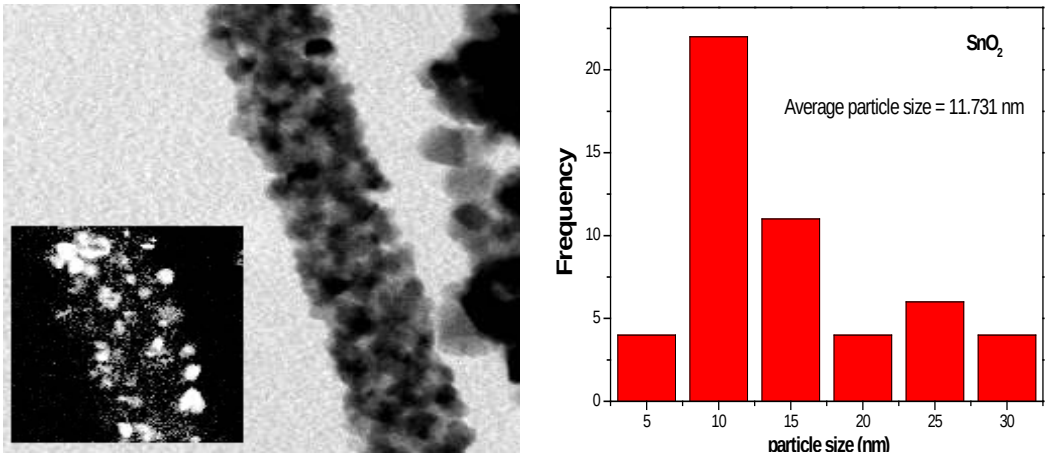

(a) (b)

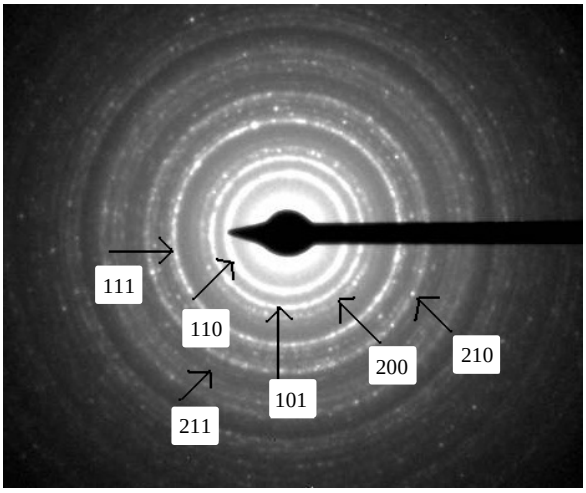

(c)

Figure 2. (a) TEM image of SnO_2 nanofiber calcined at 600˚C for 4 h. Inset: nanofiber in dark scattered surface; (b) Particle size distribution of SnO_2 nanofibers; (c) SEAD pattern of SnO_2 nanofibers (denotes diffraction facets for SnO_2).

Table 1. Comparison of inter-planer spacings (d_{hkl}) from standard tin oxide diffraction data (JCPDS file No. 77-0452) with the calculated and experimentally observed values from SAED and XRD diffractogram.

JCPDS No: 77-0452			SAED	XRD
d_{hkl} (Å)	Intensity	*h k l*	Calculated d_{hkl} (Å)	Observed d_{hkl} (Å)
3.3624	999	110	3.27	3.37
2.6643	757	101	2.699	2.65
2.3776	207	200	2.361	2.38
2.3177	33	111	ND	ND
2.1265	12	210	1.855	2.12
1.7710	515	211	1.745	1.68

One contribution varies as $1/\cos\theta$ and the other as $\tan\theta$. If both contributions are present then their combined effect should be determined by convolution. The simplification of Williamson and Hall is to assume the convolution is either a simple sum or sum of squares (see previous discussion on Sources of Peak Broadening within this section). Using the former of these then we get:

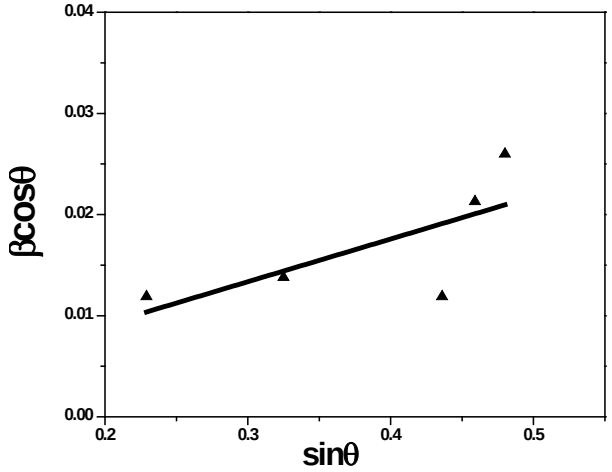

Figure 3. Williamson-Hall plot of SnO_2 nanofibers.

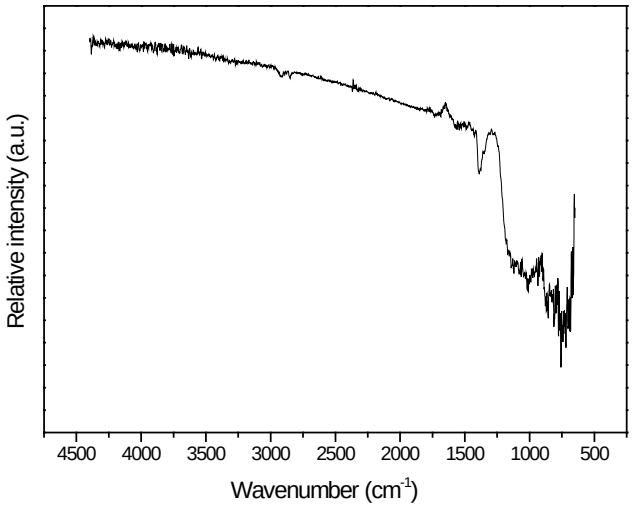

Figure 4. FT-IR spectrum of SnO_2 nanofibers.

$$\beta_{tot} = \beta_e + \beta_L = C \in \tan\theta + K\lambda/L\cos\theta \quad (5)$$

If we multiply this equation by cosθ we get:

$$\beta_{tot}\cos\theta = C \in \sin\theta + K\lambda/L \quad (6)$$

and comparing this to the standard equation for a straight line (m = slope; c = intercept)

$$y = mx + c$$

We see that by plotting β_{tot} cosθ versus sinθ we obtain the strain component from the slope (**C**ε).

3.1.3. FT-IR Analysis

Figure 4 sows the FTIR spectra of the prepared SnO_2 samples dried at 80˚C. The peaks around 1645 and 3421 cm^{-1} correspond to the bending vibrations of absorbed molecular water and the stretching vibrations of–OH groups respectively. The weak peaks at 2367 and 2907 cm^{-1} belong to the stretching vibrations of-C-H-bonds, and the ones at 1405, 1257 and 1023 cm^{-1} correspond to the bending vibrations of $-CH_2$ and $-CH_3$, which shows that a few organic groups are absorbed on the surfaces of SnO_2nanoparticles [27]. From this spectrum, it can be observed apparently at 663 cm^{-1} that strong band associated with the antisymmetric Sn-O-Sn stretching mode of the surface-bridging oxide formed by condensation of adjacent surface hydroxyl groups.

4. Conclusion

In conclusion, SnO_2 nanofibers have been produced by an electrospinning method and characterized by X-ray powder diffraction (XRD) and transmission scanning electron microscopy (TEM). The XRD result showed that SnO_2 nanofibers have tetragonal cassiterite crystalline phase. The best annealing temperature is about 600˚C. The sizes of the nanoparticles in the nanofibers estimated by TEM were found be about 11 nm while those of the nanofiber lie in the range of about 100 - 200 nm.

References

[1] Yang, P.D., Yan, H.Q., Mao, S., Russo, R., Johnson, J., Saykally, R., Morris, N., Pham, J., He, R. and Choi, H. (2002) Controlled Growth of ZnO Nanowires and Their Optical Properties. *Journal of Advanced Materials*, **12**, 323. http://dx.doi.org/10.1002/1616-3028(20020517)12:5<323::aid-adfm323>3.0.co;2-g

[2] Zhai, T.Y., Zhong, H.Z., Gu, Z.J., Peng, A.D., Fu, H.B., Ma, Y., Li, Y.F. and Yao, J.N. (2007) Manipulation of the Morphology of ZnSe Sub-Micron Structures Using CdSe Nanocrystals as the Seeds. *Journal of Physical Chemistry C*, **111**, 2980-2986. http://dx.doi.org/10.1021/jp067498x

[3] Lieber, C.M. and Wang, Z.L. (2007) Functional Nanowires. *MRS Bulletin*, **32**, 99-108. http://dx.doi.org/10.1557/mrs2007.41

[4] Li, Z., Wang, X. and Lin, T. (2014) Highly Sensitive SnO_2 Nanofiber Chemiresistors with a Low Optimal Operating Temperature: Synergistic Effect of Cu^{2+}/Au Co-Doping. *Journal of Materials Chemistry A*, **2**, 13655-13660. http://dx.doi.org/10.1039/C4TA01926A

[5] Xia, Y.N., Yang, P.D., Sun, Y.G., Wu, Y.Y., Mayers, B., Gates, B., Yin, Y.D., Kim, F. and Yan, H.Q. (2003) One-Dimensional Nanostructures: Synthesis, Characterization, and Applications. *Advanced Materials*, **15**, 353-389. http://dx.doi.org/10.1002/adma.200390087

[6] Song, X., Qi, Q., Zhang, T. and Wang, C. (2009) A Humidity Sensor Based on KCl-doped SnO_2 Nanofibers. *Sensors and Actuators B*: *Chemical*, **138**, 368-373. http://dx.doi.org/10.1016/j.snb.2009.02.027

[7] Zhang, Y., Li, J.P., An, G.M. and He, X. (2010) Highly Porous SnO_2 Fibers by Electrospinning and Oxygen Plasma Etching and Its Ethanol-Sensing Properties. *Sensors and Actuators B*: *Chemical*, **144**, 43-48. http://dx.doi.org/10.1016/j.snb.2009.10.012

[8] Zhang, Z., Shao, C., Li, X., Zhang, L., Xue, H., Wang, C. and Liu, Y. (2010) Electrospun Nanofibers of ZnO-SnO_2 Heterojunction with High Photocatalytic Activity. *Journal of Physical Chemistry C*, **114**, 7920-7925. http://dx.doi.org/10.1021/jp100262q

[9] Yang, Z., Du, G., Feng, C., Li, S., Chen, Z., Zhang, P., Guo, Z., Yu, X., Chen, G., Huang, S. and Liu, H. (2010) Synthesis of Uniform Polycrystalline Tin Dioxide Nanofibers and Electrochemical Application in Lithium-Ion Batteries. *Electrochimica Acta*, **55**, 5485-5491. http://dx.doi.org/10.1016/j.electacta.2010.04.045

[10] Yamazoe, N., Sakai, G. and Shimanoe, K. (2003) Oxide Semiconductor Gas Sensors. *Catalysis Surveys from Asia*, **7**, 63-75. http://dx.doi.org/10.1023/A:1023436725457

[11] Yamazoe, N. (1991) New Approaches for Improving Semiconductor Gas Sensors. *Sensors and Actuators B*: *Chemical*, **5**, 7-19. http://dx.doi.org/10.1016/0925-4005(91)80213-4

[12] Korotcenkov, G. (2005) Gas Response Control through Structural and Chemical Modification of Metal Oxide Films: State of the Art and Approaches. *Sensors and Actuators B*: *Chemical*, **107**, 209-232. http://dx.doi.org/10.1016/j.snb.2004.10.006

[13] Williams, D.E. and Pratt, K.F.E. (2000) Microstructure Effects on the Response of Gas-Sensitive Resistors Based on Semiconducting Oxides. *Sensors and Actuators B*: *Chemical*, **70**, 214-221. http://dx.doi.org/10.1016/S0925-4005(00)00572-4

[14] Gong, S., Liu, J., Xia, J., Quan, L., Liu, H. and Zhou, D. (2009) Gas Sensing Characteristics of SnO_2 Thin Films and Analyses of Sensor Response by the Gas Diffusion Theory. *Materials Science and Engineering B*: *Advanced Functional Solid-State Materials*, **164**, 85-90. http://dx.doi.org/10.1016/j.mseb.2009.07.008

[15] Xu, L., Dong, B., Wang, Y., Bai, X., Liu, Q. and Song, H. (2010) Electrospinning Preparation and Room Temperature Gas Sensing Properties of Porous In_2O_3 Nanotubes and Nanowires. *Sensors and Actuators B*: *Chemical*, **147**, 531-538. http://dx.doi.org/10.1016/j.snb.2010.04.003

[16] Soares, A.J. and Perry, R.J. (2010) Modeling and Simulation of a Single Tin Dioxide Nanobelt FET for Chemical Sensors. *IEEE Sensors Journal*, **10**, 235-242. http://dx.doi.org/10.1109/JSEN.2009.2032154

[17] Qiu, Y., Chen, P. and Liu, M. (2010) Evolution of Various Porphyrin Nanostructures via an Oil/Aqueous Medium: Controlled Self-Assembly, Further Organization, and Supramolecular Chirality. *Journal of the American Chemical Society*, **132**, 9644-9652. http://dx.doi.org/10.1021/ja1001967

[18] Park, J.Y., Choi, S.-W. and Kim, S.S. (2010) A Synthesis and Sensing Application of Hollow ZnO Nanofibers with Uniform Wall Thicknesses Grown Using Polymer Templates. *Nanotechnology*, **21**, Article ID: 475601. http://dx.doi.org/10.1088/0957-4484/21/47/475601

[19] Kim, I.D., Rothschild, A., Lee, B.H., Kim, D.Y., Jo, S.M. and Tuller, H.L. (2006) Ultrasensitive Chemiresistors Based on Electrospun TiO_2 Nanofibers. *Nano Letters*, **6**, 2009-2013. http://dx.doi.org/10.1021/nl061197h

[20] Wang, Y., Ramos, I. and Santiago-Aviles, J.J. (2007) Detection of Moisture and Methanol Gas Using a Single Electrospun Tin Oxide Nanofiber. *IEEE Sensors Journal*, **7**, 1347-1348. http://dx.doi.org/10.1109/JSEN.2007.905045

[21] Wang, G., Ji, Y., Huang, X., Yang, X., Gouma, P.I. and Dudley, M.J. (2006) Fabrication and Characterization of Polycrystalline WO_3 Nanofibers and Their Application for Ammonia Sensing. *The Journal of Physical Chemistry B*, **110**, 23777-23782. http://dx.doi.org/10.1021/jp0635819

[22] Liu, Z., Sun, D.D., Guo, P. and Leckie, J.O. (2007) An Efficient Bicomponent TiO_2/SnO_2 Nanofiber Photocatalyst Fabricated by Electrospinning with a Side-by-Side Dual Spinneret Method. *Nano Letters*, **7**, 1081-1085. http://dx.doi.org/10.1021/nl061898e

[23] Li, S., Shao, C., Liu, Y., Tang, S. and Mu, R. (2006) Nanofibers and Nanoplatelets of MoO_3 via an Electrospinning Technique. *Journal of Physics and Chemistry of Solids*, **67**, 1869-1872. http://dx.doi.org/10.1016/j.jpcs.2006.04.017

[24] Kim, I.D., Hong, J.M., Lee, B.H., Kim, D.Y., Jeon, E.K., Choi, D.K. and Yang, D.J. (2007) Dye-Sensitized Solar Cells Using Network Structure of Electrospun ZnO Nanofiber Mats. *Applied Physics Letters*, **91**, Article ID: 163109. http://dx.doi.org/10.1063/1.2799581

[25] Formo, E., Lee, E., Campbell, D. and Xia, Y. (2008) Functionalization of Electrospun TiO_2 Nanofibers with Pt Nanoparticles and Nanowires for Catalytic Applications. *Nano Letters*, **8**, 668-672. http://dx.doi.org/10.1021/nl073163v

[26] Chen, H., Wang, N., Di, J., Zhao, Y., Song, Y. and Jiang, L. (2010) Nanowire-in-Microtube Structured Core/Shell Fibers via Multifluidic Coaxial Electrospinning. *Langmuir*, **26**, 11291-11296. http://dx.doi.org/10.1021/la100611f

[27] Gnanam, S. and Rajendran, V. (2010) Preparation of Cd-Doped SnO_2 Nanoparticles by Sol-Gel Route and Their Optical Properties. *Journal of Sol-Gel Science and Technology*, **56**, 128-133. http://dx.doi.org/10.1007/s10971-010-2285-7